SIMULATION OF THE DAMAGE MECHANISMS OF GLASS FIBER REINFORCED POLYPROPYLENE BASED ON MICRO SPECIMENS AND 1:1 MODELS OF THEIR MICROSTRUCTURE

Sascha Fliegener[1], Tobias Kennerknecht[1] and Matthias Kabel[2]
[1] Fraunhofer Institute for Mechanics of Materials (IWM), Freiburg, Germany
Email: sascha.fliegener@iwm.fraunhofer.de, Web Page: http://www.iwm.fraunhofer.de
[2] Fraunhofer Institute for Industrial Mathematics (ITWM), Kaiserslautern, Germany

Keywords: micromechanical damage modeling, short fiber reinforced plastics, in situ testing

Abstract
Fiber reinforced thermoplastics are considered as promising candidates to enable the mass production of lightweight components. To assure their structural application, precise methods to describe their mechanical behavior are mandatory. However, the modeling of the damage behavior of the thermoplastic matrix under multiaxial stress states within the microstructure still poses enormous challenges. In order to capture the in situ behavior of the matrix and the fiber-matrix interface, a novel methodology is applied in our work. Micro tensile specimens, which are manufactured from 100 µm thin slices of the material's cross section, are tested up to their failure. A corresponding finite element mesh which precisely depicts the individual microstructure of each specimen is reconstructed based on computer tomographic scans. Due to the dimensions of the specimens being sufficiently small, the position and orientation of each fiber can be directly mapped to the model. Micromechanical simulations are performed to separate the contributions of the matrix, the interface and the fibers to the global response of the specimens. It is shown that the stress-strain response of two specimens with a strongly different microstructure can be accurately captured by our simulations under application of the same material parameters. Furthermore, the damage evolution within the microstructure of the simulations and the experiments is visualized and compared.

1. Introduction

Discontinous fiber reinforced thermoplastics are widely used in semi-structural parts, since they offer attractive stiffness and strength to weight ratios and can be produced by cost-efficient mass production techniques as injection and compression molding. At least for short fiber reinforcements, state-of-the-art integrative simulation techniques from mold filling to structural simulation are quite sophisticated as long as the predictions are restricted to the elastic properties. The modeling of the nonlinear, elasto-plastic behavior still poses enormous challenges. Nevertheless, some approaches also address this issue with a degree of accuracy which is sufficient for most engineering applications. However, the modeling of the evolution of damage within the microstructure represents a major limitation. In contrast to unidirectional layers of continuous fibers, where different damage modes can be distinguished based on the load direction in relation to the fiber orientation (e.g. the failure mode concept of Cuntze), no such clear differentiation can be made for discontinuous fiber reinforced plastics mainly due to the strong local variation of the microstructure (fluctuations of fiber orientation and density). To develop micromechanical models of the damage evolution within such a microstructure, it is necessary to characterize the damage evolution on exemplary specimens. First approaches to visualize and to understand the damage mechanisms of short fiber composites were made by Sato *et al.* by means of evaluation of SEM images, taken at multiple times during the loading of a bending specimen [1]. The specimen was polished to observe the evolution of damage in the vicinity of fibers which were cut at the specimen surface. They also applied acoustic emission methods and estimated the stress levels in the matrix, the fibers and the interface close to the point of failure of the composite [2]. In more recent publications, in situ microtomography is applied to study the damage evolution of tensile specimens of a glass fiber reinforced thermoplastic [3]. In this context, also the damage accumulation during fatigue loading was characterized by image correlation techniques applied on computertomographic scans to evaluate the fraction of micro voids [4].

Excerpt from ISBN 978-3-00-053387-7

In our work, we follow a different route by the applying a combined experimental-numerical procedure. Micro tensile specimens are prepared from the cross section of a compression molded plate (glass fiber reinforced polypropylene). Due to the microscopic dimensions (200 µm width, 100 µm thickness) of the gauge section, the position and angle of each fiber can be directly mapped to a corresponding finite element (FE) model and it is no longer necessary to use statistical distributions (e.g. a fiber orientation tensor) to describe the microstructure. Thus, no uncertainty with respect to the geometry exists and the corresponding simulations of each specimen can be used to visualize and to evaluate the individual damage mechanisms. Furthermore, the parameters of the constitutive laws of the matrix and the interface can be inversely determined. In our work, we demonstrate the feasibility of our methodology by the modeling of two specimens with a strongly different microstructure and damage evolution. The preparation of the specimens and the in situ testing is outlined in the experimental section. In the modeling section, the generation of the FE models and the parameters of the simulations are described and finally, the experimental results are compared to the simulations.

2. Experimental methods

2.1 Specimen preparation

First, thin slices of the material were prepared from the cross section of compression molded plates of glass fiber reinforced polypropylene with the dimensions of 400 x 400 x 3 mm³. Details on the investigated material can be found in [5]. For this purpose, stripes with approx. 5 x 3 x 1 mm³ were cut from the plates with a slicing disk. In the following, the stripes were polished multiple times with diamond suspension of decreasing grain size and a final grain size of 3 µm. First, one side of the stripe was treated until a suitable quality of the surface could be ensured by evaluation of microscope images. Then, the specimen was flipped to its backside and the procedure was repeated until a final thickness of approx. 100 µm was reached. The contour of the specimens with a hourglass-shaped gauge section was then finished by a computer controlled milling machine. The dimensions of the gauge section are 800 µm (length), 200 µm (width) and 100 µm (thickness).

2.2 Micro tests

In situ testing was performed under application of the apparatus shown in Fig. 1. More details of the test setup and used components can be found in [6]. The experiments were carried out at an average strain rate of $1.25 \cdot 10^{-3}$ 1/s, yielding a total time of 695 s for specimen 1 and 380 s for specimen 2. The load was measured with a load cell with 5 N capacity at a frequency of 10 Hz. Images of the specimen surface were acquired by a microscope with an optical magnification factor of 10, a frequency of 1 Hz and a camera resolution of 1.81 px/µm. An image correlation technique based on a custom script [7] was applied to obtain the value of engineering strain for each image by evaluation of two sets of markers outside the damage localization zone. The results are presented together with the simulations in Fig. 4-7.

3 Simulation

3.1 Reconstruction of the microstructure

A corresponding finite element mesh for each individual specimen was created. For our studies, we selected two specimens with a strongly different microstructure. Specimen 1 features a fiber volume fraction of approx. 5 % and failed by normal fracture in the middle of the hourglassed gauge section. In contrast, specimen 2 has a volume fraction of approx. 15 % and failed in shear mode. The microstructure of both specimens in the form of a 3D model was manually reconstructed based on microscope images of the front and backside of the specimen before testing. Additionally, computertomographic (CT) scans were acquired at the specimens after failure. The models are compared to the specimens in Fig. 2 and 3. It was not possible to acquire CT scans of each specimen before testing since approx. 25 specimens were tested in total and only two were selected for the modeling as described next.

Excerpt from ISBN 978-3-00-053387-7

3.2 Micromechanical simulations

To perform the FE simulations, the 3D models (Fig. 2 and 3) were meshed with linear tetrahedral elements of approx. 5 µm edge length and a total element count of approx. $1.5 \cdot 10^6$ for both models. The simulations were performed by Abaqus Explicit under assumption of isotropic elastic properties for the glass fibers. The polypropylene matrix is assigned to elastic-plastic properties and damage in the form of a classical von Mises plasticity model with isotropic, multilinear hardening and a strain-based damage model. A cohesive contact formulation between the fibers and the matrix and a traction-separation law was activated for the simulations which account for interface failure. In contrast, tie constraints were used for the simulations which consider a perfect bonding. Displacement boundary conditions were applied at the borders of the model. To evaluate the strain, two node sets were defined outside the damage localization zone in the middle of the gauge sections with the same distance as the markers used for the image correlation procedure of the experiments. The engineering strain was then calculated from the averaged displacements of both node sets. A parametric model was set up with the target to minimize the deviation between numerical and experimental stress-strain curves. The software LS-OPT was applied for the automatic parameter optimization procedure. Finally, the values of the multilinear hardening of the matrix, the damage energy of the matrix and the damage energy of the interface were determined by the optimization procedure. Moreover, it was ensured by visual observations that the evolution of damage of the virtual specimens was similar to the experimental findings (see Fig. 4-5). The applied material parameters can be found in Table 1.

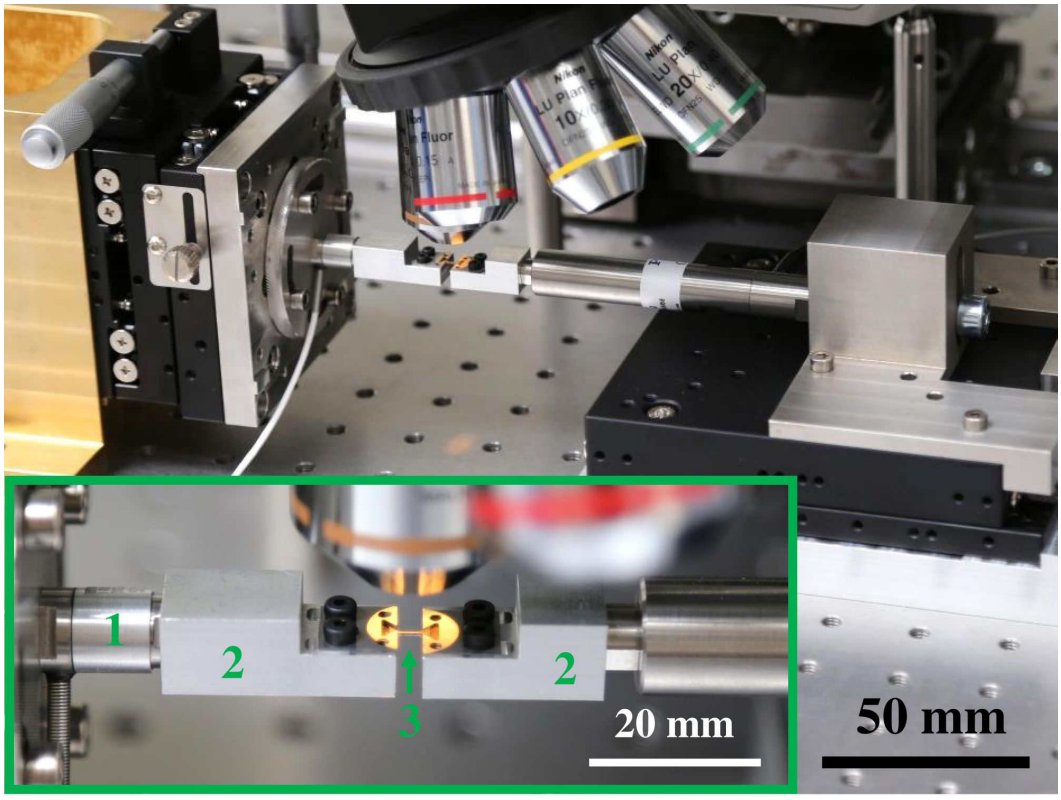

Figure 1. Micromechanical in situ test setup with load cell (1), specimen clamps (2) and specimen (3). More details are given in [6].

Excerpt from ISBN 978-3-00-053387-7

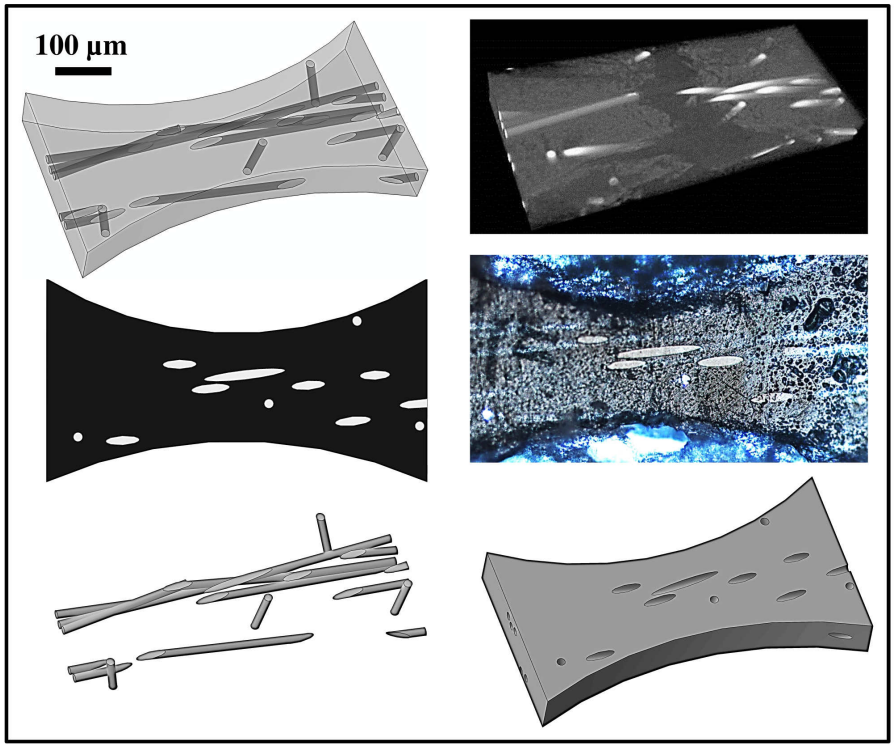

Figure 2. Microstructure of specimen 1 (5 vol-%): transparent 3D model (top left), CT scan after fracture (top right), surface of the 3D model (middle left), surface of the specimen, microscope image (middle right), fibers of the 3D model (bottom left), matrix of the 3D model (bottom right)

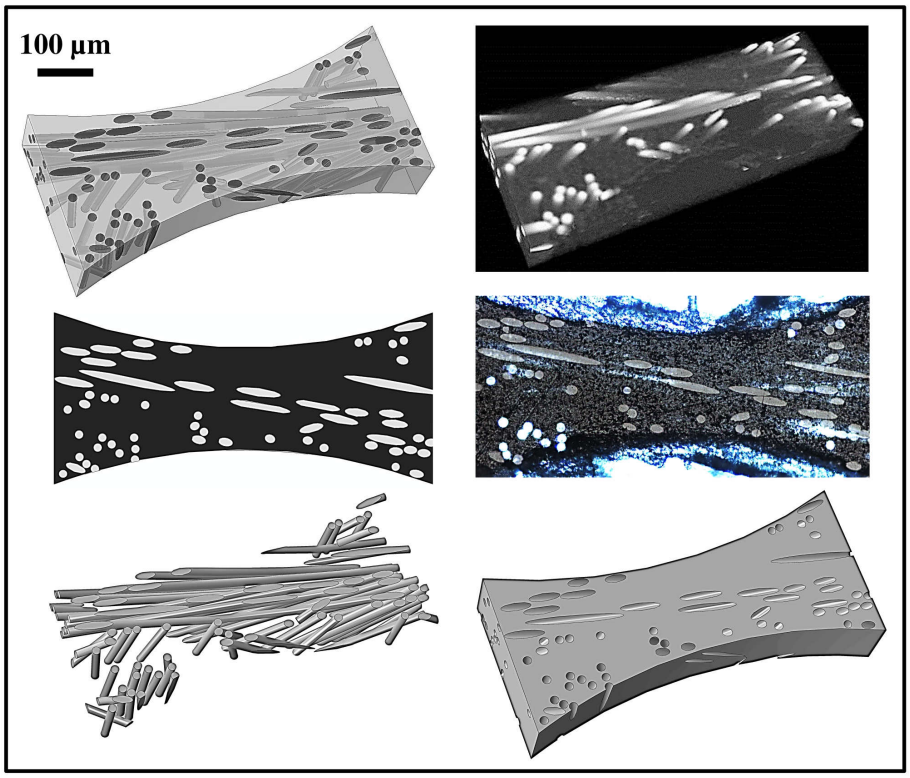

Figure 3. Microstructure of specimen 2 (15 vol-%): transparent 3D model (top left), CT scan after fracture (top right), surface of the 3D model (middle left), surface of the specimen, microscope image (middle right), fibers of the 3D model (bottom left), matrix of the 3D model (bottom right)

Excerpt from ISBN 978-3-00-053387-7

4. Results

In Fig. 4 and 5, microscope images of the specimen surface are compared to contour plots of equivalent plastic strain of the corresponding simulations at multiple times during the experiment / simulation. The simulations account for matrix and interface damage and are based on the same material parameters specified in Table 1. An excellent agreement between experiments and simulations can be observed. The different failure modes (normal and shear fracture) of both specimens are accurately captured. In Fig. 6 and 7, the stress-strain curves of both specimens and corresponding simulations are compared. In general, a good agreement between the numerical and experimental curves can be seen. It is remarkable that specimen 1 features only approx. half of the maximum stress of specimen 2 and the relation of maximum strains is vice versa. A similar trend is existent for the numerical curves. For specimen 1, the effect of interface damage on the stress-strain curves is rather low. However, the evolution of damage (Fig. 4) exclusively agrees to the experimental observations if interface damage is activated. For specimen 2, the failure strain can only be reached by consideration of interface damage. Up to the stress peak, the agreement between the simulation which only accounts for plasticity and the experiment is even better, but predicts a far too low maximum strain.

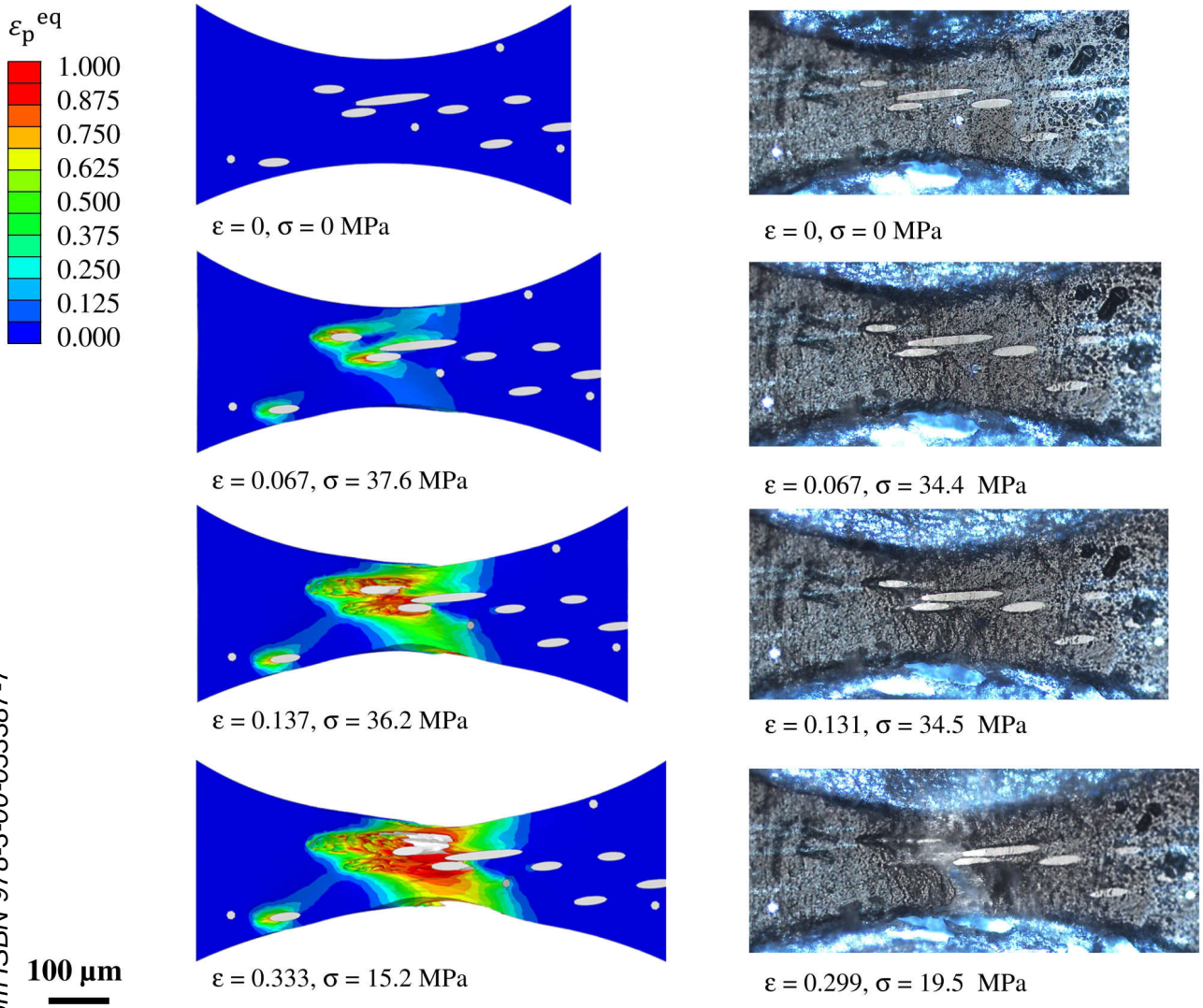

Figure 4. The evolution of deformation and damage at the microscale for specimen 1 (5 vol-%) visualized by contour plots of the equivalent plastic strain and microscope images of the specimen surface during the in situ testing.

Excerpt from ISBN 978-3-00-053387-7

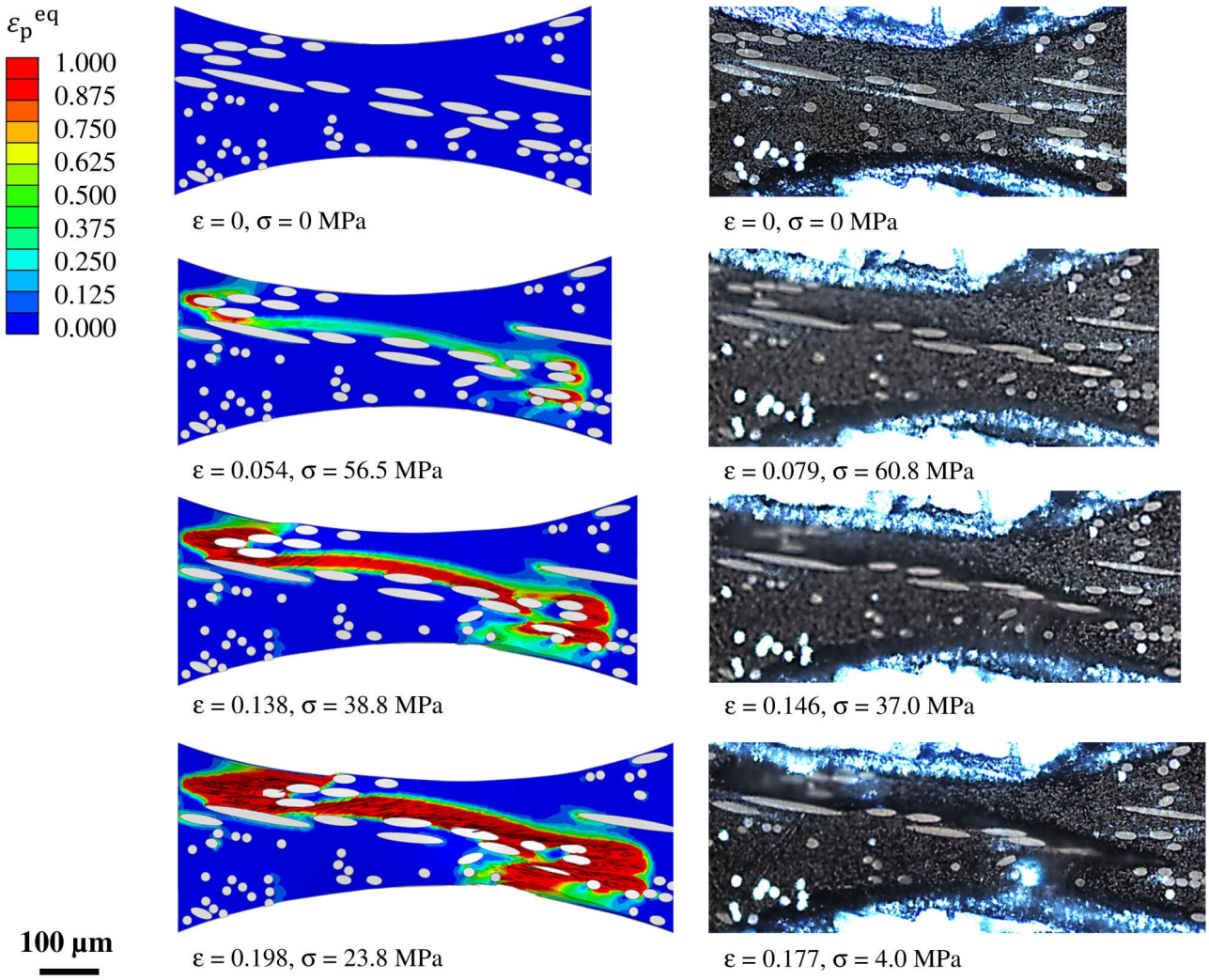

Figure 5. The evolution of deformation and damage at the microscale for specimen 2 (15 vol-%) visualized by contour plots of the equivalent plastic strain and microscope images of the specimen surface during the in situ testing.

5. Conclusions

A novel combined experimental-numerical procedure to model the damage behavior of fiber reinforced plastics was presented. The procedure is based on micro specimens of sufficiently small dimensions so that the position of each fiber can be directly mapped to a corresponding finite element mesh. The damage evolution of two exemplary specimens with a strongly different microstructure and thus, strongly different failure modes can be reproduced to a high degree of accuracy, using the same constitutive material parameters for both simulations. In future, our methodology can be applied to precisely adjust the material parameters - including the evolution of damage - by inverse simulations.

Excerpt from ISBN 978-3-00-053387-7

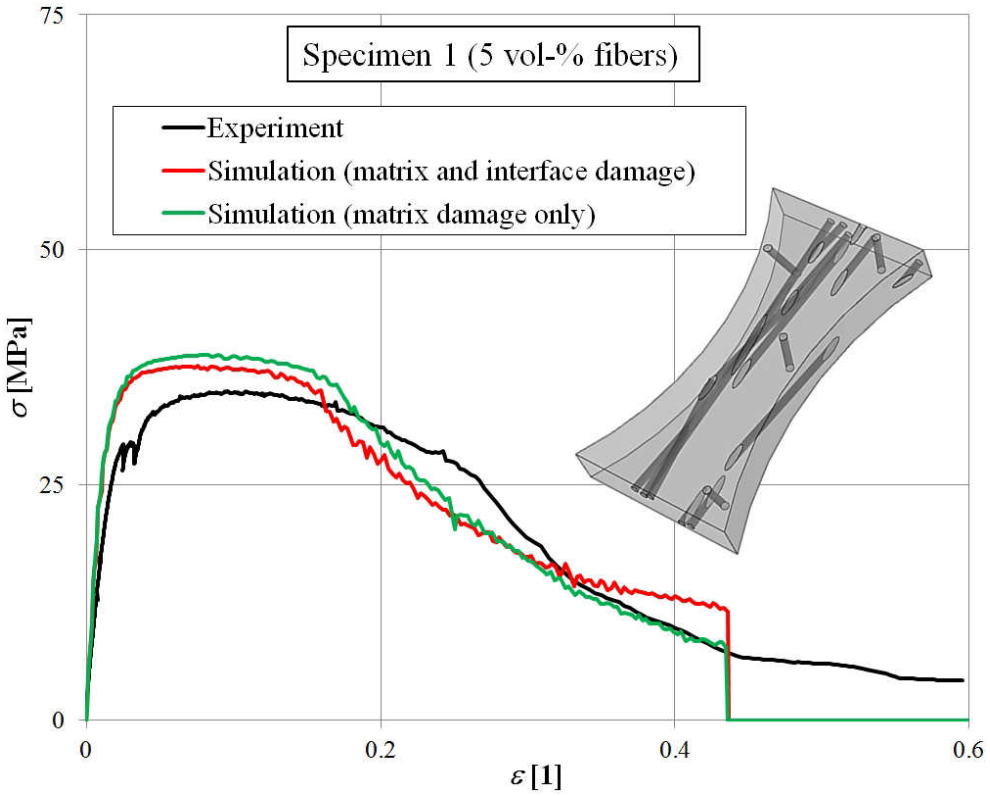

Figure 6. Stress-strain curves of specimen 1 (5 vol-%) compared to two simulation variants accounting for matrix and interface damage / matrix damage only.

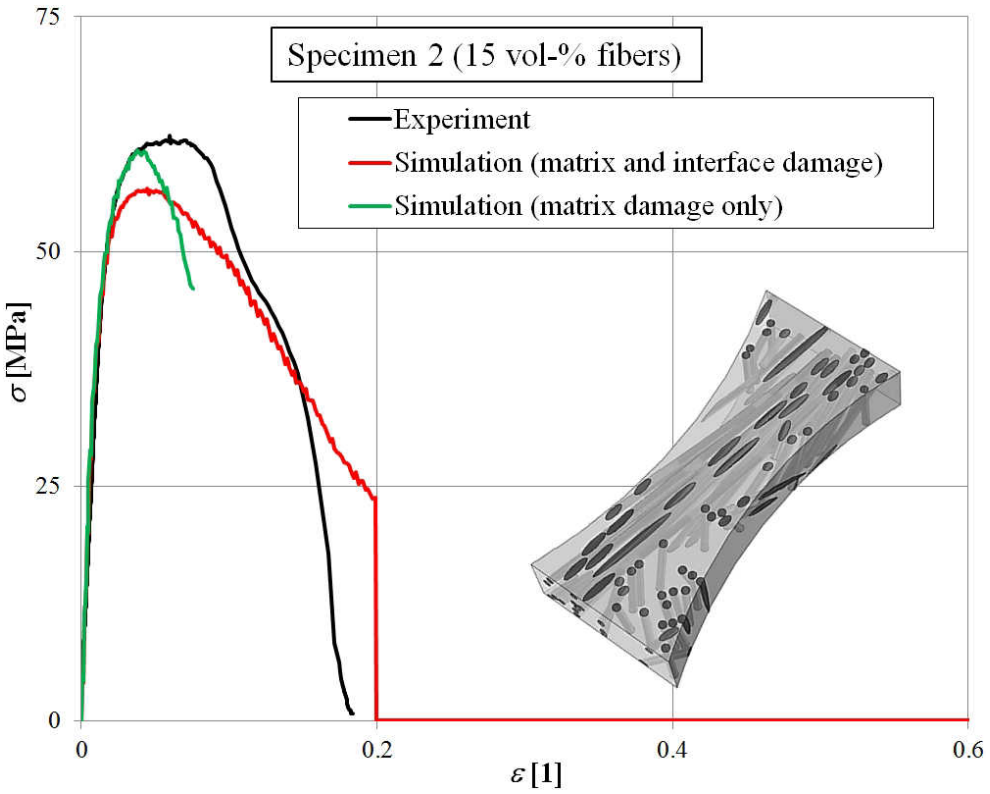

Figure 7. Stress-strain curves of specimen 2 (15 vol-%) compared to two simulation variants accounting for matrix and interface damage / matrix damage only.

Excerpt from ISBN 978-3-00-053387-7

Table 1. Material properties for the micromechanical simulations

Property	Value	Unit	Description
E_f	$7.2 \cdot 10^4$	MPa	Young's modulus of the glass fibers
ν_f	0.22	-	Poisson's ratio of the glass fibers
E_m	1250	MPa	Young's modulus of the polypropylene matrix
ν_m	0.35	-	Poisson's ratio of the polypropylene matrix
$(\sigma_Y/\varepsilon_p)_1$	14.20 / 0.0000	MPa / -	First value pair of equivalent yield stress / eq. plastic strain of the multilinear, isotropic hardening of the matrix
$(\sigma_Y/\varepsilon_p)_2$	20.12 / 0.0104	MPa / -	Second value pair of equivalent yield stress / eq. plastic strain of the multilinear, isotropic hardening of the matrix
$(\sigma_Y/\varepsilon_p)_3$	22.50 / 0.0204	MPa / -	Third value pair of equivalent yield stress / eq. plastic strain for of multilinear, isotropic hardening of the matrix
ε_p^{ini}	2	-	Eq. plastic strain for damage initiation of the matrix
G_f	0.1	mJ	Damage evolution energy of the matrix (linear softening)
K	10^6	N/mm	Stiffness of the traction-separation law of the interface, no mode-dependence, uncoupled stiffness matrix (cohesive contact)
δ_{ini}	$2 \cdot 10^{-4}$	mm	Separation at damage initiation of the traction-separation law of the interface, no mode-dependence, quadratic form of the initiation criterion (cohesive contact)
δ_f	10^{-3}	mm	Separation at failure of the traction-separation law of the interface, no mode-dependence, linear softening (cohesive contact)

References

[1] Sato N, Kurauchi T, Sato S, Kamigaito O. Microfailure behavior of randomly dispersed short fibre reinforced thermoplastic composites obtained by direct SEM observation. *Journal of Materials Science 26* (1991), pp. 3891-3898

[2] Sato N, Kurauchi T, Sato S, Kamigaito O. Mechanism of fracture of short glass fibre-reinforced polyamide thermoplastic. *Journal of Materials Science 19* (1984), pp. 1145-1152

[3] Rolland H, Saintier N, Robert G. Damage mechanisms in short glass fibre reinforced thermoplastic during in situ microtomography tensile tests. *Composites Part B 90* (2016), pp. 365-377

[4] Cosmi F, Bernasconi A. Micro-CT investigation on fatigue damage evolution in short fibre reinforced polymers. *Composites Science and Technology 79* (2013), pp. 70-76

[5] Fliegener S, Luke M, Gumbsch, P. 3D microstructure modeling of long fiber reinforced thermoplastics. *Composites Science and Technology 104* (2014), pp. 136-145

[6] Kennerknecht T. Fatigue of Micro Molded Materials - Aluminum Bronze and Yttria Stabilized Zirconia. PhD thesis, Karlsruhe Institute of Technology (KIT), 2014, ISBN 978-3-7315-0293-7, DOI 10.5445/KSP/1000043832

[7] Senn M. Digital Image Correlation and Tracking. MathWorks® File Exchange (2015), http://www.mathworks.com/matlabcentral/fileexchange/50994-digital-image-correlation-and-tracking

Excerpt from ISBN 978-3-00-053387-7